

STATE OF THE ART RADIOMETER STANDARDS FOR NASA'S EARTH OBSERVING SYSTEM

Carlos R Jorquera, Virginia G. Ford, Valerie G. Duval, Carol J. Bruegge
Jet Propulsion Laboratory, California Institute of Technology
4800 Oak Grove Drive MS 303-210 Pasadena, CA 91109
T: (818) 354-3546 F: (818) 393-6047 EMail: Carlos.R.Jorquera@jpl.nasa.gov

Raj Korde
International Radiation Detectors
2545 W. 237th Street, Suite 1 Torrance, CA 90505

The Multi-Angle imaging SpectroRadiometer (MISR), to be launched in 1998, is one of five instruments on NASA's first Earth Observing System (EOS) platform. The 3% (1σ) absolute radiometric calibration requirement is considered challenging, particularly since it must be maintained through the five-year mission life. The instrument requirements have led to the development of an On-Board Calibrator (OBC) consisting of diffuse panels and photodiode-based radiometric standards. Although used extensively in national standard laboratories, MISR will be the first in-orbit instrument to utilize Spectralon calibration targets, and the first instrument to establish a radiometric scale in orbit using detector-based standards. The team has adopted the nomenclature High Quantum Efficiency (HQE) technology to refer to the implementation of 100% internal quantum efficient photodiodes in a trapped configuration. Filtered HQE radiometers are being utilized in the preflight calibration phase to calibrate the flat-field source (integrating sphere). In order to provide an element of continuity between the preflight and post-launch calibrations (and to provide the most accurate characterization of camera illumination levels during flight), HQE radiometers will also be used to characterize solar-reflected light from the diffuse calibration targets during the mission. In addition, radiation-resistant photodiodes will be utilized as part of the OBC. These have an extended space-life time over the HQEs, and allow for an uncertainty estimation of the calibration when the HQE and radiation-resistant photodiode data sets are compared.

INTRODUCTION

The Multi-angle Imaging SpectroRadiometer (MISR) features nine pushbroom cameras, recording in four spectral bands to provide global images of the Earth's surface every nine days, at the Equator (see Fig. 1). Data from these 36 channels are spatially registered during ground processing to provide measurements through path lengths of 1.0, 1.1, 1.4, 2.0, and 3.0 (0° , $\pm 26.1^\circ$, $\pm 45.6^\circ$, $\pm 60.0^\circ$, and $\pm 70.5^\circ$ in view angle). The availability of an angular measurement for each scene pixel makes these data unique. Spatial sampling ranges from 275 m (250 m cross-track in the nadir) to 1.1 km (1.0 km cross-track in the nadir), depending on the "camera-configuration", or on-board pixel averaging mode used prior to transmission of the data. The spectral band shape will nominally be Gaussian and centered at 443, 555, 670, and 865 nm. Bandwidth is specified to be 25, 15, 15,

and 25 nm, respectively, for the four bands (Gaussian full-width half-maximum). The Gaussian profile, used in conjunction with a Lyot birefringent cube, will provide depolarization of the incoming light, and allow the instrument to be polarization insensitive. MISR data will enable investigations into cloud, aerosol, and surface properties.

Throughout the five year mission, MISR must maintain absolute radiometric accuracy to within $\pm 3\%$ (1 σ) over high reflectance, spatially uniform scenes. The instrument must be polarization insensitive to $\pm 1\%$ and radiometrically accurate to better than 2% at 24 pixels distance from a high-contrast edge (e.g. not be limited by image blur and scatter beyond this amount). Geometric specifications include ± 250 m along-track/ ± 500 m (2 σ) cross-track co-registration for the nine camera images. The temporal stability requirement is 2% drift per year, or less.

To achieve the radiometric requirements, MISR utilizes an On-Board Calibrator (OBC). Included is a pair of diffuse panels. These are required to have a high, near-Lambertian reflectance. While not in use the panels are stowed and protected. The panels will be deployed at monthly time intervals and used to direct sunlight into the cameras, filling their fields-of-view and providing a through-the-optics calibration. Over the North Pole, a plate will swing aftward to diffusely reflect sunlight into the fields-of-view of the aftward-looking and nadir cameras. Over the South Pole, the other plate will swing forward for calibration of the forward-looking and nadir cameras. The nadir camera will provide a link between the two sets of observations. Cumulative space exposure time (deploy time) for each panel is expected to be less than 100 hours over the mission life.

SpectralonTM has been selected as the material to be used as the MISR in-orbit calibration targets. Spectralon is a product of Labsphere (North Sutton, New Hampshire), and is composed of pure polytetrafluoroethylene (PTFE, 'or Teflon) polymer resin that is compressed into a hard porous white material. Spectralon targets are widely used in laboratory and ground/field operations as a reflectance standard. MISR has provided for the flight qualification of this material.

As diffusers in general are subject to UV degradation and contamination, they in themselves are not typically used as a radiometric standard. In the case of MISR, the calibration targets will be monitored by three types of radiometers, each possessing a different photodiode design: radiation-resistant diodes and two types of High Quantum Efficiency (HQE) diodes. The radiation-resistant detectors are designed to be insensitive to otherwise damaging space radiation. They are expected to degrade no more than 2% for the 5-year mission. The HQE sensors are tailored for optimum performance within two spectral regions. The "Blue" HQE photodiodes achieve a nearly 100% internal quantum efficiency in the first two MISR spectral bands (443 and 555 nm), while the "Red" HQE diodes are intended for the other two bands (670 and 865 nm).

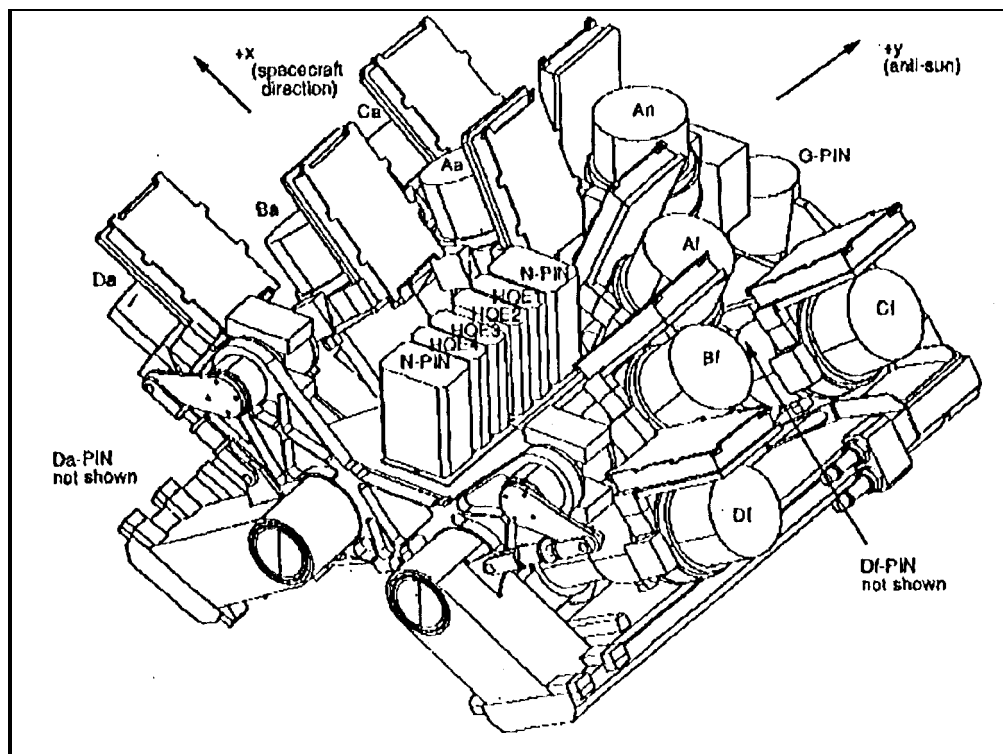


Figure 1. MISR optical bench. Four forward looking (Af, Bf, Cf, Df), four aftward looking (Aa, Ba, Ca, Da), and one nadir camera. PIN refers to the radiation-resistant radiometers.

The utilization of photodiode standards during flight to characterize diffuse panel radiance allows the MISR instrument to be calibrated without reliance on source irradiance knowledge. For this reason stray-light and Earth-shine do not contribute to the calibration uncertainty, provided they are uniform sources across the panel. Also, MISR will calibrate at several radiometric levels, by acquiring data as the sun passes through a varying Earth-atmospheric path during the first minute of calibration. This activity would not be possible if reliance on panel radiance from a solar-irradiance and earth atmosphere-transmittance model were required.

During the mission, MISR also plans to conduct semi-annual ground calibration campaigns, utilizing field measurements and higher resolution sensors (aboard aircraft or in-orbit platforms) to provide a check of the on-board hardware. These ground calibration campaigns are limited in number, but believed key to validation of the flight calibration as provided by the OBC.

HQE AND RADIATION- RESISTANT RADIOMETER DESIGNS

Both the HQE and radiation-resistant radiometers are composed of three main sections: a hermetically sealed assembly containing the photodiodes; an electronic assembly housing a trans-impedance amplifier; and a precision baffle assembly which defines the light cone incident on the sensors. The hermetically sealed assembly consists of a multi-layer ceramic package which conducts the diode signals through electrical traces, from the hermetically sealed volume to the unscaled electronics assembly. On the outside of the ceramic, the traces are terminated in pins which are oven-braised onto the ceramic. The amplifier interfaces directly to these pins.

On the sealed side of the ceramic, a frame is oven-braised in a circle enclosing the volume. Photodiode sub-assemblies are bonded to the ceramic. Covers are placed on the frame and laser-welded in place to form a hermetic seal. The hermetic volume is purged through a tube (which is oven-braised onto the ceramic), then backfilled with Argon. The purge tube is crushed then sealed with epoxy. The hermetic package provides a stable environment, and eliminates the potential for damage due to humidity or contaminants. As both the diodes and camera CCDs will be hermetically sealed in their packages, it is expected that filter shifts, although predicted to be small, will be of the same magnitude and direction for the calibration and camera systems alike,

The baffle assemblies consist of tubes having precision apertures at both ends that define a field-of-view of approximately 8° . The apertures are precision made using photolithography and chemical etching techniques, and manufactured to a diameter uncertainty of 2 μm . The distance between these apertures is tightly defined by the tubes and retaining structures to an accuracy of $\pm 0.05\%$. This yields an uncertainty in the $A\Omega$ product (function of collective area and solid angle) of less than 0.5%. The inside of the tubes is baffled to reduce stray-light reflections from reaching the diodes. Structure is provided at both ends of the tube. On the outside end, the structure holds the precision aperture and provides threaded holes for the aperture retainer. On the inside end, the structure holds the inner precision aperture, interfaces with the cover of the hermetically sealed package, and ensures that the light baffles inside the tube are held tightly,

HQE Radiometer Configuration

Within the hermetic package, each of the HQE photodiodes is in a light-trap configuration where three photodiodes are arranged optically in series, as shown in figure 2. The light reflected from one diode is collected by the next, such that all the incoming signal is detected, resulting in near 100% quantum efficiency. In addition, the configuration is arranged so that the path of the incoming light is made to switch planes once entering. This is done to minimize the polarization sensitivity of the trap.

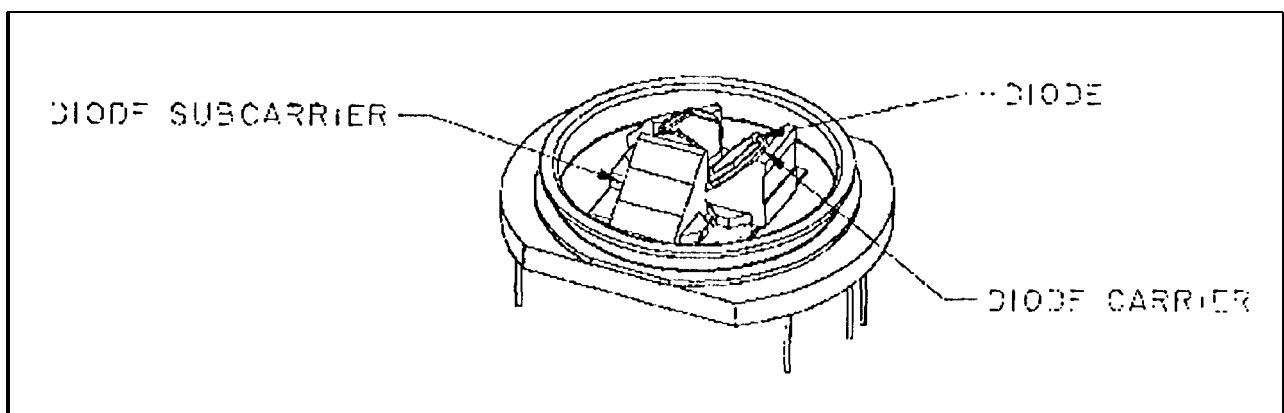


Figure 2. HQE photodiode light-trap.

The individual diodes are bonded onto ceramic carrier disks that protect them during testing and further assembly, and provide isolated metallized pads for electrical contacts. Wires are ball-bonded from the diodes to the pads. These diode assemblies are then bonded onto ceramic sub-carriers. The sub-carriers are triangular in shape and hold the diode assemblies at the angles required to

produce the light-trap configuration. Additionally, the sub-carriers have internal electrical traces that carry the diode signals from the diode carriers to the bottom of the subcarrier. The diode carriers are bonded with conductive epoxy to the sub-carrier, making the electrical connections for the signals. The sub-carriers are bonded to a metallic ground plane with conductive epoxy. The positive signal connection is formed by ball bonding a wire from a pad on the sub-carrier to a pad on the surface of the HQE ceramic package.

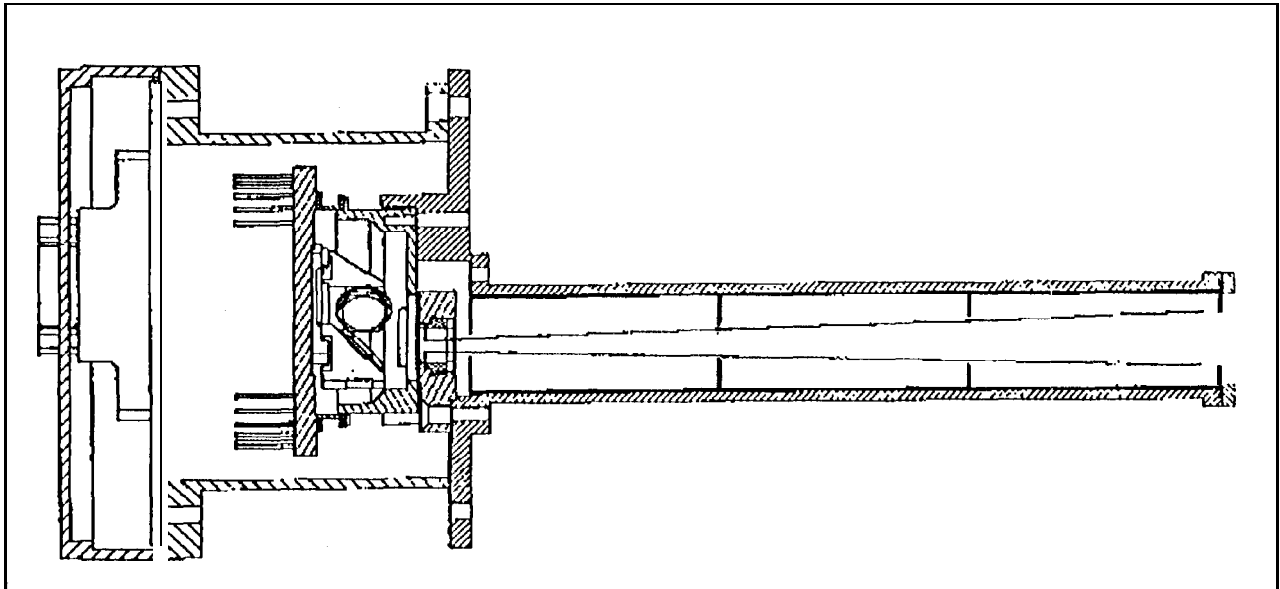


Figure 3. HQE radiometer configuration.

The cover of the HQE hermetic package has a window that is soldered in place. A single spectral filter per package is bonded to this window, and four such packages provide coverage at the four MISR wavelengths. The HQE baffle assembly consists of one tube holding inner and outer precision apertures. The flange of the base of the light tube provides structure for attaching the electronics and for interfacing with the optical bench of the instrument (see Fig. 3).

Radiation-Resistant Radiometer Configuration

The radiation-resistant photodiode package has four diodes inside the hermetic volume, with each diode filtered to a different MISR spectral band. As with the HQE assembly, radiation-resistant diodes are first bonded onto ceramic carrier disks. These diode carriers are then bonded into cavities in the ceramic base. Electrical connections are made by bonding the diode carriers with conductive epoxy to the package. The filters are bonded to the ceramic package directly on top of the diodes. Finally, the cover, which in this case has four soldered windows, is laser-welded to the package frame.

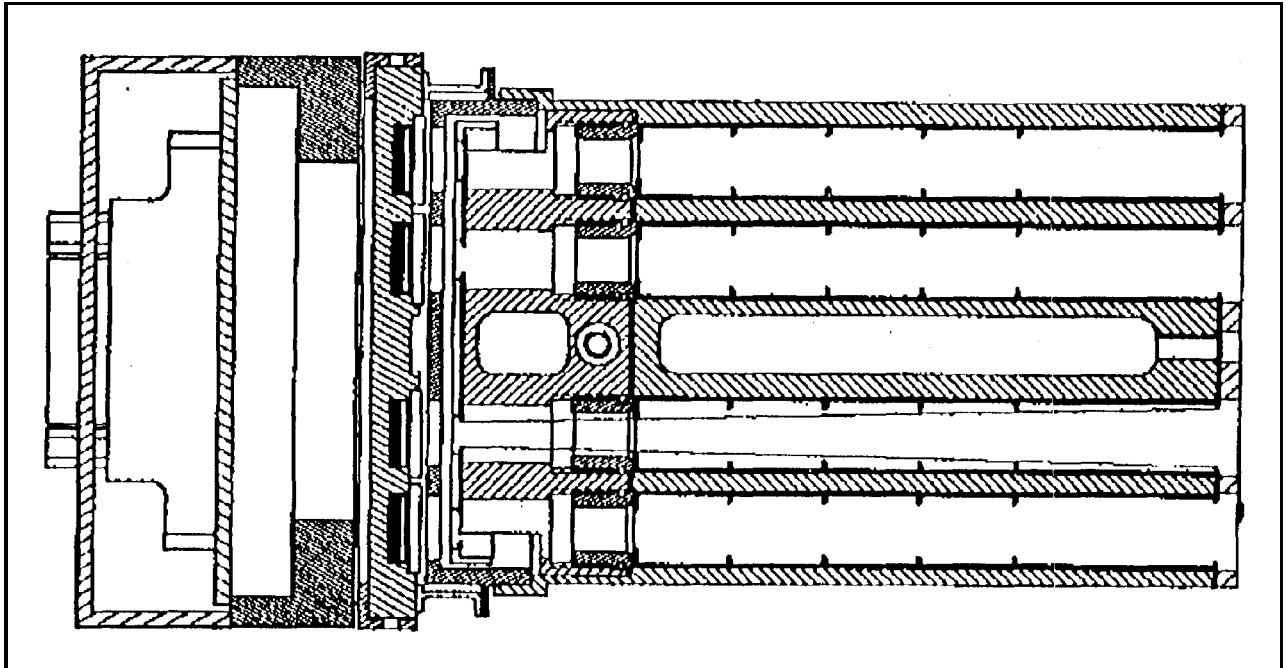


Figure 4. Radiation-resistant radiometer configuration,

The radiation-resistant baffle assembly has four tubes, each holding inner and outer precision apertures. The flange of the tube assembly is attached to the package cover with screws. The package and baffle combination is then bonded into a ring that attaches to a mounting plate. This mounting plate interfaces to the electronics assembly and the optical bench of the instrument (see Fig. 4).

On the instrument, five radiation-resistant radiometers will be used. Two will view in the nadir direction, two in the forward and aft 70.5° camera directions, and one detector assembly will be mechanized on a goniometric arm to monitor the angular reflectance properties of the calibration panels (see Fig. 1).

PHOTODIODE DESIGNS

Specifications common to the HQE and radiation-hard photodiodes include a surface reflectance loss of less than 25% and a signal-to-noise ratio greater than 500 at full scale. (For the MISR cameras, full scale has been defined as a scene with an equivalent reflectance of 1, Equivalent reflectance, ρ_{eq} , provides a measure of radiance, L_λ , as normalized by the exo-atmospheric solar irradiance, $E_{0\lambda}$, at wavelength λ , and is defined by $\rho_{eq} = \pi L_\lambda / E_{0\lambda}$). The HQE photodiodes have been further specified to have an internal quantum efficiency (IQE) exceeding 0.995, to have a linearity of response better than 99.8% over an equivalent reflectance range of 0.05 to 1.0, and stability to within $\pm 2\%$ through the first six months of flight. For the radiation-hard photodiodes, the specifications are an external QE of greater than 0.30, linearity to better than 99.5%, and stability to within $\pm 2\%$ through the five-year mission. With these photodiode specifications it is estimated that the diffuse panel radiance can be determined to within $\pm 1\%$ uncertainty. Panel illumination non-uniformities, relative bi-directional reflectance factor (BRF) knowledge of the panel, and difference

between the photodiode and CCD response functions bring the total estimated error in calibration to *3%.

Blue HQE Photodiode Design- MISR Bands 1-2

The detector design implemented for MISR spectral bands 1 and 2 (443 and 555 nm) consists of a shallow-junction n-on-p photodiode fabricated on 4" diameter P-P+ epitaxial (epi) silicon wafers. The epi silicon layer for these wafers has a thickness of approximately 25 μm and possesses a resistivity of greater than 1 $\Omega\cdot\text{cm}$. Phosphorus diffusion is carried out to obtain a shallow junction 0.1 to 0.25 μm deep (see Fig. 5). Through careful processing this design is capable of achieving dynamic resistances of upwards of 1 $\text{G}\Omega$, resulting in detectors with very low noise performance. Additionally, in order to minimize signal losses due to front-surface reflections, the silicon dioxide anti-reflection coating is optimized for MISR bands 1 and 2. This is accomplished by thinning the coating down to about 80 nm following completion of the diffusion.

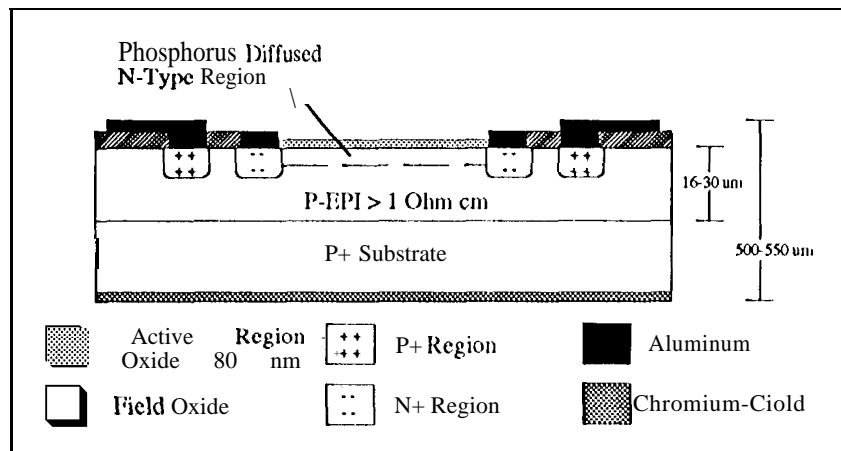


Figure 5. Blue HQE photodiode design.

This design offers several advantages over other earlier proposals, in particular, a more stable and lower noise performance that does not require biasing for high QE operation. This is a very significant improvement over the inversion-layer photodiode [1], which is the more traditional choice for this particular spectral range, and which until not long ago [2] was the only detector type that could achieve IQEs large enough which allowed it to be used in the fabrication of absolute radiometric standards [3].

Red HQE Photodiode Design- MISR Bands 3 and 4

The Red HQE detectors intended for MISR bands 3 and 4 (670 and 865 nm) are p-on-n photodiodes fabricated on 4" float zone silicon wafers, again with a resistivity greater than 1 $\Omega\cdot\text{cm}$ (Fig. 6). The p-n junction was created by a specific boron ion implantation process which minimizes the front surface dead region of the photodiode, thereby achieving very high IQE, even at the shorter wavelengths [4]. As was the case for the blue HQE diodes, dynamic resistances greater than

1 G Ω were also obtained for the red HQE diodes, The optimal SiO₂ anti-reflection coating thickness used for these wavelengths was 128 nm.

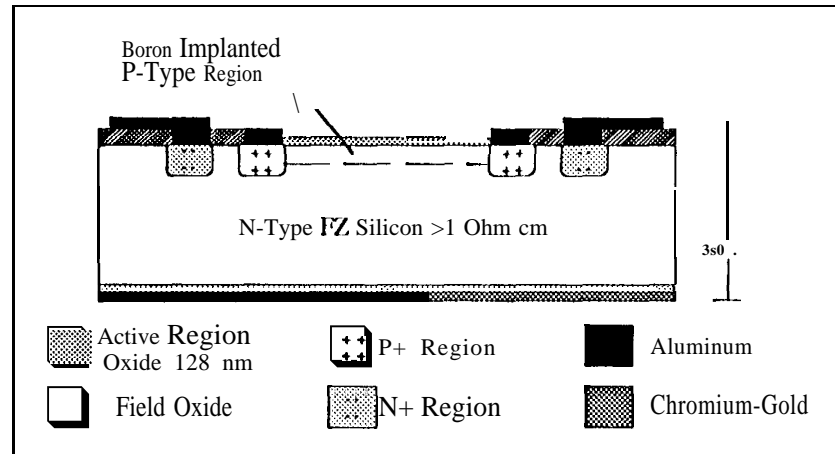


Figure 6. Red HQE photodiode design.

Radiation-Hard Photodiode Design

In order to achieve the radiation-hardness required, and at the same time obtain highest possible external QE, six different types of radiation-hard photodiodes were fabricated to attain the optimal trade-off. Three types of these detectors were built on p-p+ epitaxial wafers, each type having one of three possible epi layer thicknesses of 5, 15, or 25 μm (same structure as Fig. 5 except for the cpi thickness). The remaining three diode types were fabricated on Silicon Oxide Insulator (SOI) wafers (with a buried oxide thickness in the range of 250 to 1000 rim), and similarly, each type had one of three possible active Silicon thicknesses: 5, 10, or 18 μm . Because the active Silicon thickness for the radiation-hard detectors was limited to a maximum of 25 μm , IQE was expected to be lowest for MISR band 4. Hence, the anti-reflection coating was optimized for this spectral region in the same way as for the Red HQEs. In addition, as with the HQE diodes, a dynamic resistance of greater than 1 G Ω was also another goal of this design.

DETECTOR PERFORMANCE

IQE and Reflectance Measurements

These measurements were performed by following the technique used in a previous study [5]. Essentially, two types of light-trapping 100% QE detectors were used as absolute standards: an inversion-layer QED-200 trap made by United Detector Technologies; and a Graseby Optonics QED-1 50 trap composed of Hamamatsu photodiodes. The QED-200 was the reference for MISR bands 1 and 2, while the QED-1 50 was best suited for bands 3 and 4. A light-tight fixture was fabricated to place the photodiode under test at 45° from the opening to the QED-200, and readings were acquired for the reflected signal, the photodiode signal, and the total incoming signal measured by an additional QED-200 and the QED-150. From these measurements it was then possible to directly calculate both the front surface reflectance (at 45°) and the IQE for the photodiodes.

The results presented some surprises. First of all, the Red HQE diode response showed to be extremely high ($> 99\%$) for wavelengths below 600 nm, which is generally not expected from p-n photodiode architectures. This indicates that the Red HQE photodiodes lack the front dead region normally found in p-n diodes. Unfortunately this performance was short lived. In a span of little over a month following fabrication, the IQE for these devices dropped down to 90% at 420 nm, and down to 97.7% at 552 nm (Fig. 7), indicating that there are still serious issues of stability to resolve. It is of importance to note that this IQE degradation was not due to humidity effects since all photodiodes were kept within a dry nitrogen purge.

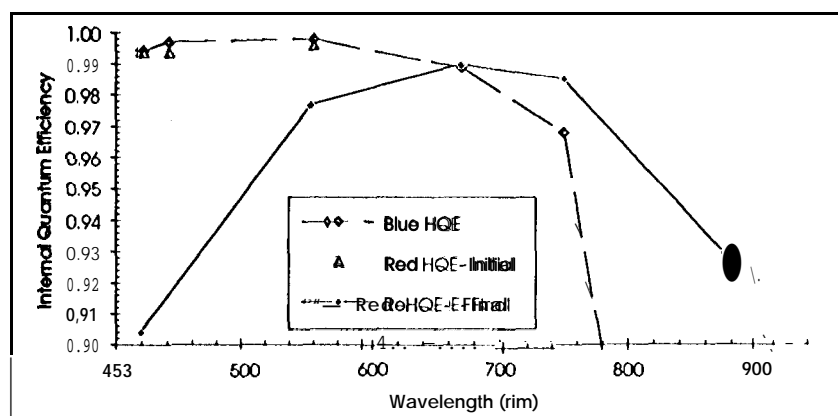


Figure 7. Typical Blue and Red HQE photodiode IQE.

Another unexpected result pertaining to the Red HQE sensors was that the IQE at the longer wavelengths showed not to be as high as required, only about 92% at 875 nm. This may be attributed in part to the fact that the foundry used for building these photodiodes is primarily dedicated to IC fabrication, and therefore their processing is not particularly tailored for obtaining long minority carrier life times, as is critical for these detectors. Currently, additional foundries which specialize on detectors are being involved in further photodiode fabrication runs in the hopes of solving this problem.

The Blue HQE detectors generally showed acceptable performance, although their IQEs at 420 nm were approximately 99.4%, which was not quite as high as desired (Fig. 7).

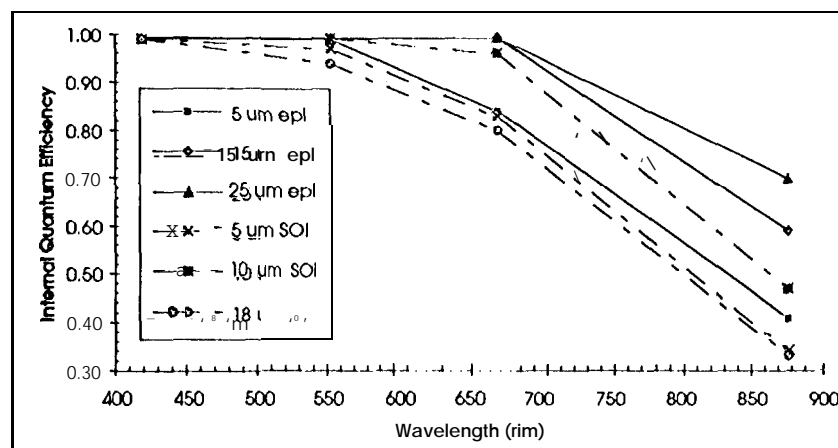


Figure 8. Typical IQE for all Radiation-hard photodiode types.

The radiation-hard photodiode IQE results met more closely with expectations. First of all, the detectors fabricated on epi wafers showed very comparable performance to the Blue HQE diodes in MISR bands land 2. This was as expected since the only difference between the rad-hard designs on epi wafers and the Blue HQE design was the epi thickness involved. Towards the longer wavelengths, their IQEs were strong functions of the active silicon thickness of each rad-hard diode, also as expected (Fig. 8). The one exception to this were the S01 diodes with an active silicon thickness of 18 μm , which had the lowest IQE in all bands. This was due to the fact that this particular wafer was of a different type than the other S01 wafers, and additionally, was of lower quality.

Front surface reflectance for all photodiode types was found to be at worst 20%, for spectral regions not targeted by anti-reflection coating optimization, and at best 10%, for those regions which were optimized.

IV Characterization, Shunt Resistance, and Shunt Capacitance Measurements

Current vs. bias voltage (IV) curves were obtained for all photodiodes. From these, the dynamic resistance at zero bias (shunt resistance) was calculated for each diode using data points near zero volts. In a separate step, shunt capacitance was also obtained. All three measurements were performed at ambient temperature, which was generally about 26° Celsius. The shunt resistance for all photodiodes was determined to be very nearly 1 G Ω , with the exception of the Red HQE diodes, for which it was approximately 10 G Ω . It is of importance to point out that the operating temperature for all these detectors, once in flight, is expected to be approximately 10° C. Taking into account the shunt resistance temperature coefficient for these diodes, which was measured approximately to be a 10% decrease per degree C increase, it is expected that the shunt resistance for all photodiodes will be about three times as large in-flight as has been measured at room temperature. Therefore, these sensors are expected to have excellent signal-to-noise ratios.

SPACE RADIATION EFFECTS

Fully characterized photodiode samples of each type were selected for proton radiation damage testing. The fluences for all other charged particles during the mission are expected to be negligible. The photodiodes were irradiated at four proton energies: 0.1, 0.5, 1.0, and 5.0 MeV. Different photodiodes of each type were exposed to each of the four energies, and an additional set were exposed to all four energies. The fluence for each proton energy level was chosen according to what is expected for the five year flight mission times a factor of three as an error margin: 4.8×10^7 , 3.2×10^7 , 1.2×10^8 , and 6.0×10^8 $\frac{\text{PROTONS}}{\text{cm}^2}$. Following irradiation, characterization measurements were repeated to determine the amount of induced performance degradation.

The results were a great deal more favorable than originally expected. All radiation-hard and Blue HQE photodiodes showed no noticeable IQE changes at any of the exposed proton energies, even at 875 nm. The radiation-hard photodiodes built on epi wafers (and the Blue HQE devices for that matter) were expected to be extremely radiation insensitive at the shorter wavelengths [6]. Similar results were also expected for the detectors fabricated on S01 wafers, although no data was

available on these. At the longer wavelengths IQE variations were expected to be a function of the detector's active Silicon thickness. It was very encouraging to see that the predicted fluences were too low to produce noticeable changes even at the longer wavelengths for the rad-hard and Blue HQE sensors.

Data obtained from the Red HQE devices matched more closely what was expected. No IQE changes were detected in the first two MISR bands (420 nm and 552 nm), while for bands 3 and 4 (670 nm and 875 nm) IQE drops of 2% and 11%, respectively, were observed. Additionally, this degradation was only measured at the proton energy of 5.0 MeV, indicating that only the damage towards the rear volume of the photodiodes was significant.

ACKNOWLEDGMENTS

The authors would like to thank Charles Cruzan, Don Dunn, and Nick Mardesich for their key roles in all aspects of the packaging effort.

The research described in this paper was carried out by the Jet Propulsion Laboratory, California Institute of Technology, under a contract with the National Aeronautics and Space Administration.

Reference herein to any specific commercial product, process, or service by trade name, trademark, manufacturer, or otherwise, does not constitute or imply its endorsement by the United States Government or the Jet Propulsion Laboratory, California Institute of Technology.

REFERENCES

- [1] Hansen, T. "Silicon UV Photodiode Using Natural Inversion Layers," *Phys. Scripta*, vol. 18 (1978): p. 471.
- [2] Korde, R., Geist, J. "Stable, High Quantum Efficiency UV-Enhanced Silicon Photodiodes by Arsenic Diffusion," *Solid State Electronics* vol. 30 (1987): pp. 89-92.
- [3] Zalewski, E. F., Duda, C.R. "Silicon photodiode device with 100% external quantum efficiency," *Applied Optics* vol. 22(1983): pp. 2867-2873.
- [4] Korde, R., Geist, J. "Quantum Efficiency Stability of Silicon Photodiodes," *Applied Optics* vol. 26 (1989): pp. 5284-5290.
- [5] Jorquera, C. R., Bruegge, C., Duval, V. "Evaluation of high quantum efficiency silicon photodiodes for calibration in the 400 nm to 900 nm spectral region," in *SPIE Vol. 1762 Infrared Technology XVIII*, 1992, pp. 135-144.
- [6] Korde, R., Cable, J. S., Canfield, L.R. "100% Internal Quantum Efficiency Silicon Photodiodes with One Gigarad Passivating Silicon Dioxide," *IEEE Trans. in Nuclear Science* vol. 40 no. 6 (1993): pp. 1655-1659.